약학박사 학위 논문

In Vitro and *In Vivo* Evaluation of Puerarin on Hepatic Cytochrome P450-Mediated Drug Metabolism

간 사이트크롬 P450 약물 대사에서 Puerarin 이 미치는 영향에 대한 연구

2014 년 8 월

서울대학교 대학원

약학과 약제과학 전공

김 상 범

ABSTRACT

In Vitro and *In Vivo* Evaluation of Puerarin on Hepatic Cytochrome P450-Mediated Drug Metabolism

Sang-Bum Kim

Department of Pharmaceutics

The Graduate School

Seoul National University

Dissertation director: Prof. Dae-Duk Kim

Puerarin (PU, 8-β-D-glucopyranosyl-7-hydroxy-3-(4-hydroxyphenyl)-4H-1-benzopyran-4-one) is a major pharmacological component of *Puerariae Radix*, the root of *Pueraria lobata* (Willd) Ohwi. The effect of PU on hepatic

cytochrome P450 (CYP)-mediated drug metabolism in rats and human was investigated. The *in vitro* CYP inhibitory effect of PU in human and rat liver microsomes (HLM and RLM, respectively) was evaluated using the following model CYP substrates; *i.e.*, phenacetin (PHE) for CYP1A, diclofenac (DIC) for CYP2C, dextromethorphan (DEX) for CYP2D, and testosterone (TES) for CYP3A. The *in vivo* pharmacokinetics of intravenous and oral buspirone (BUS), a probe substrate for CYP3A, was studied with single simultaneous intravenous co-administration of PU in rats. In the *in vitro* CYP inhibition study, the rate of disappearance of TES was significantly reduced in the presence of 10-μM PU, while that of other CYP substrates was not significantly affected in both HLM and RLM, suggesting that PU inhibits the *in vitro* hepatic CYP3A-mediated metabolism in the human and rat systems (IC_{50} = 15.5 ± 3.9 μM). After intravenous administration of BUS with single simultaneous co-administration of intravenous PU at a dose of 10 mg/kg in rats, the AUC was increased while CL decreased. When BUS was orally administered in rats with the 10 mg/kg intravenous PU co-administration, both AUC and F were significantly increased. Therefore, results of the *in vitro* microsomal and *in vivo* pharmacokinetic studies suggest the possible inhibition of hepatic CYP3A-mediated drug metabolism by PU administration, potentially leading to metabolism-mediated herb–drug interactions with clinical significance.

Key words: puerarin, cytochrome P450, buspirone, hepatic metabolism, pharmacokinetics

Student number: 2010-30463

CONTENTS

List of Tables

Part I. *In Vitro* and *In Vivo* Evaluation of Puerarin on Hepatic Cytochrome P450-Mediated Drug Metabolism

Part II. Metabolic interactions of magnolol with cytochrome P450 enzymes in human and rat liver microsomes

List of Figures

Part I. *In Vitro* and *In Vivo* Evaluation of Puerarin on Hepatic Cytochrome P450-Mediated Drug Metabolism

Part II. Metabolic interactions of magnolol with cytochrome P450 enzymes in human and rat liver microsomes

Part I

In Vitro and *In Vivo* Evaluation of Puerarin on Hepatic Cytochrome P450-Mediated Drug Metabolism

1.1. ABSTRACT

Puerarin (PU, 8-β-D-glucopyranosyl-7-hydroxy-3-(4-hydroxyphenyl)-4H-1-benzopyran-4-one) is a major pharmacological component of *Puerariae Radix*, the root of *Pueraria lobata* (Willd) Ohwi. The effect of PU on hepatic cytochrome P450 (CYP)-mediated drug metabolism in rats and human was investigated. The *in vitro* CYP inhibitory effect of PU in human and rat liver microsomes (HLM and RLM, respectively) was evaluated using the following model CYP substrates; *i.e.*, phenacetin (PHE) for CYP1A, diclofenac (DIC) for CYP2C, dextromethorphan (DEX) for CYP2D, and testosterone (TES) for CYP3A. The *in vivo* pharmacokinetics of intravenous and oral buspirone (BUS), a probe substrate for CYP3A, was studied with single simultaneous intravenous co-administration of PU in rats. In the *in vitro* CYP inhibition study, the rate of disappearance of TES was significantly reduced in the presence of 10-μM PU, while that of other CYP substrates was not significantly affected in both HLM and RLM, suggesting that PU inhibits the *in vitro* hepatic CYP3A-mediated metabolism in the human and rat systems (IC_{50} = 15.5 ± 3.9 μM). After intravenous administration of BUS with single simultaneous co-administration of intravenous PU at a dose of 10 mg/kg in rats, the AUC was increased while CL decreased. When BUS was orally administered in rats with the 10 mg/kg

intravenous PU co-administration, both AUC and F were significantly increased. Therefore, results of the *in vitro* microsomal and *in vivo* pharmacokinetic studies suggest the possible inhibition of hepatic CYP3A-mediated drug metabolism by PU administration, potentially leading to metabolism-mediated herb–drug interactions with clinical significance.

Key words: puerarin, cytochrome P450, buspirone, hepatic metabolism, pharmacokinetics

Abbreviations: PU, puerarin; PHE, phenacetin; DIC, diclofenac; DEX, dextromethorphan; TES, testosterone; BUS, buspirone; HLM, human liver microsome; RLM, rat liver microsome; CYP, cytochrome P450; AUC, total area under the plasma concentration–time curve from time zero to time infinity; CL, time-averaged total body clearance; Vss, apparent volume of distribution at steady state; F, extent of absolute oral bioavailability.

1.2. INTRODUCTION

Herbal extracts are commonly used as alternative medicines (Bent 2008). A national survey in the United States reported that 18.9% of the adult population consumed herbs to treat medical illnesses within the past 12 months (Bardia, Nisly et al. 2007). Some herbal extracts were reported to modulate the activity of drug metabolizing enzymes, leading to metabolism-mediated herb-drug interactions (Zhou, Gao et al. 2003; Kennedy and Seely 2010). Among the various drug metabolizing enzymes, cytochrome P450 monooxygenase (CYP) plays a major role in phase I drug metabolism, and more than 85% of marketed drugs are known to be metabolized by the CYPs (Rendic 2002). Thus, several studies have addressed the CYP-mediated interactions between prescribed drugs and herbs with clinical significance as follows: Naringin, naringenin and furanocoumarins in *Citrus paradisi* (grapefruit) inhibited hepatic and intestinal CYP3A4 activity, enhancing the bioavailability of buspirone (BUS), carbamazepine, saquinavir, sildenafil, and simvastatin (Tassaneeyakul, Guo et al. 2000; Girennavar, Jayaprakasha et al. 2007); hyperforin and quercetin in *Hypericum perforatum* (St. John's wort) induce the expression and activity of CYP1A2, 2C9, 2C19, 2E1, and 3A4, reducing the efficacy of indinavir, digoxin, midazolam, and atorvastatin (Komoroski, Zhang et al. 2004; Mason 2010);

ginkgolides and quercetin in *Ginkgo biloba* also induce CYP2C19 activity, reducing the efficacy of omeprazole (Yin, Tomlinson et al. 2004; Mohamed and Frye 2010). As shown in these reports, examining the CYP-mediated herb-drug interactions and their pharmacokinetic mechanisms could be crucial for the optimal design of drug and herb-based therapies.

Puerarin (PU, 8-β-D-glucopyranosyl-7-hydroxy-3-(4-hydroxyphenyl)-4H-1-benzopyran-4-one) is a major pharmacologic component of *Puerariae Radix*, the root of *Pueraria lobata* (Willd) Ohwi (Fig. **1**). Intravenous formulation of PU at a dose of 400–600 mg/day is currently prescribed for the treatment of cardiovascular disease in China (Wang, Wu et al. 2006). PU is metabolized primarily *via* UDP-glucuronosyltransferases (UGT) 1A1 in human liver microsomes (Luo, Cai et al. 2012), and its oral absorption is very low in human (Wang, Wu et al. 2006). However, most of its pharmacokinetic properties including major elimination route in animals and human remains unclear. A few studies on the relatively long-term and indirect effect of PU on the activity of CYPs did reveal that multiple intravenous injections of PU at a dose of 400 mg/day for 10 days inhibited CYP2D6 activity and induced CYP1A2 activity in eighteen healthy Chinese male volunteers (Zheng, Chen et al. 2010). Moreover, the induction of CYP1A1/2, 2A1, 2C11, and 3A1 activities was observed at 24 h after the intragastric administration of PU at a dose of 200 mg/kg in rats (Guerra,

Speroni et al. 2000). However, little information is currently available on the *in vitro* and *in vivo* CYP-mediated drug metabolism in animals or human with PU administration.

Herein, the direct effect of PU on hepatic CYP-mediated drug metabolism in rats and human through *in vitro* CYP inhibition study using human and rat liver microsomes (HLM and RLM, respectively) with model CYP substrates was examined. The *in vivo* pharmacokinetics of BUS, a probe substrate for CYP3A4 in human and CYP3A1/2 in rats, with PU administration was also evaluated.

1.3. MATERIALS AND METHODS

Materials

PU, PHE, DIC, DEX, and BUS were purchased from Sigma–Aldrich Co. (St. Louis, MO, USA). TES was purchased from Tokyo Chemical Industry Co. (Tokyo, Japan). The purity of all purchased compounds was higher than 98.0%. HLM, RLM and nicotinamide adenine dinucleotide phosphate (NADPH) regenerating system were purchased from BD-Genetech (Woburn, MA, USA). Other chemicals were of reagent grade or high-performance liquid chromatography (HPLC) grade.

In Vitro CYP Inhibition Study in HLM and RLM

In vitro CYP inhibition study using HLM and RLM was conducted according to the manufacturer's protocol using BD-UltraPool^{TM} HLM 150 (150-donor pool) and BD-Gentest^{TM} Pooled male RLM (Sprague–Dawley (SD) rats). To evaluate the effect of PU on CYP-mediated metabolic activity, the disappearance of the following model CYP substrates in HLM and RLM was determined in the presence of 10-μM PU: PHE for CYP1A2 in human and CYP 1A1/2 in rats (10 μM), DIC for CYP2C9 in human and CYP2C11 in rats (5 μM), DEX for CYP2D6 in human and CYP2D1/2 in rats (5 μM), and TES for CYP3A4 in

human and CYP3A1/2 in rats (30 μM). At 0, 20, 40, and 60 min after starting the metabolic reaction, 100 μL of microsome was sampled and transferred into a clean 1.5-mL eppendorf tube containing 200-μL acetonitrile to terminate the metabolic reaction. After vortex-mixing and centrifugation at 16,000 *g* for 10 min, 100-μL aliquot of the supernatant was stored at –70°C freezer until HPLC analysis. The IC_{50} values of PU for the inhibition of metabolic reactions of the model CYP substrates in RLM were determined by nonlinear regression according to Hill equation using GraphPad Prism 5.01 (GraphPad Software, San Diego, CA). Control samples (with no inhibitor) were assayed in each analytical run.

***In vitro* metabolism of PU in RLM**

To evaluate the CYP-mediated metabolism of PU itself, the disappearance of PU at various concentrations (5, 10, 20, and 50 μM) was determined in RLM. At 0 and 60 min after starting the metabolic reaction, 100 μL of microsome was sampled and transferred into a clean 1.5-mL eppendorf tube containing 100-μL acetonitrile to terminate the metabolic reaction. After vortex-mixing and centrifugation at 16,000 *g* for 10 min, 100-μL aliquot of the supernatant was stored at –70°C freezer until HPLC analysis.

Animals

Protocols for the animal studies were approved by the Institutional Animal Care and Use Committee of Seoul National University (date of approval, 22/07/2013; approval number, SNU-130722-1). Male SD rats (7–9 weeks old and weighing 200–250 g) were purchased from Orient Bio, Inc. (Seongnam, Korea). They were maintained in a clean room (Animal Center for Pharmaceutical Research, College of Pharmacy, Seoul National University) at a temperature of 20–23°C with 12-h light (07:00–19:00) and dark (19:00–07:00) cycles, and a relative humidity of 50 ± 5%. The rats were housed in metabolic cages (Tecniplast, Varese, Italy) under filtered, pathogen-free air, with food (Agribrands Purina, Korea; Pyeongtaek, Korea) and water available *ad libitum*.

***In vivo* pharmacokinetic study in rats**

Femoral vein and artery of rats were cannulated with polyethylene tube (Clay Adams, Parsippany, NJ, USA) 4 h before administration of drug (Kim, Cho et al. 2013), while rats were anesthetized with zoletil (20 mg/kg, intramuscular). In the pharmacokinetic study of BUS, rats were given a single intravenous dose (10 mg/kg) or oral dose (30 mg/kg) of BUS (dissolved in normal saline), with or without single simultaneous intravenous PU (dissolved in a vehicle composed of 30% ethanol, 60% PEG 400 and 10% 1N NaOH) at a dose of 10 mg/kg. An

approximately 150-μL aliquot of blood sample was collected *via* the femoral artery at 0, 2, 5, 15, 30, 60, 90, 120, and 150 min after intravenous injection and at 0, 2, 5, 10, 20, 30, 60, 90, 120, and 150 min after oral administration. In the pharmacokinetic study of PU, rats were given a single intravenous dose (10 mg/kg) of PU with single simultaneous intravenous BUS (10 mg/kg) or oral BUS (30 mg/kg). An approximately 150-μL aliquot of blood sample was collected *via* the femoral artery at 0, 2, 5, 30, 45, 60, and 90 min. After the centrifugation of blood sample at 16,000 *g* at 4^{o}C for 10 min, a 50-μL aliquot plasma sample was stored in a –70^{o}C freezer until HPLC analysis.

HPLC analysis

The concentrations of PU, PHE, DIC, DEX, TES, and BUS in the microsomal and plasma samples were determined as previously described with slight modifications (Yan, Wang et al. 2006; Reyes-Gordillo, Muriel et al. 2007; Zhang, Liu et al. 2008; Jurica, Konecny et al. 2010). A 50-μL aliquot of plasma was deproteinized with a 100-μL acetonitrile. After vortex-mixing and centrifugation at 16,000 *g* for 10 min, the supernatant was transferred to a clean eppendorf tube, and dried under nitrogen gas at room temperature. The residue was reconstituted with 100-μL mobile phase and a 70-μL aliquot was injected into a reversed phase HPLC column (C18 Gemini NX; 150 mm length × 4.6 mm i.d.; particle size, 5

μm; Phenomex, USA). The prepared 100-μL microsomal samples were directly injected into the HPLC column. The mobile phase was a mixture of 20-mM phosphate monobasic solution (PH 2.4, solvent A) and acetonitrile (solvent B). For PHE, the following gradient system was used: solvent A of 70 v/v% to 30 v/v% during 0–8 min; solvent A of 70 v/v% during 8–11 min. For DIC, the following gradient system was used: solvent A of 81 v/v% to 18 v/v% during 0–6 min; solvent A of 45 v/v% during 6–8 min. For DEX, the following gradient system was used: solvent A of 55 v/v% to 45 v/v% during 0–8 min; solvent A of 80 v/v% during 8–10 min. For BUS, the mobile phase was 80-v/v% solvent A and 20-v/v% solvent B. For PU, the mobile phase was 88-v/v% solvent A and 12-v/v% solvent B. For TES, the mobile phase was composed of 50-v/v% solvent C (deionized distilled water 95%, acetonitrile 5%, TFA 0.1%) and 50-v/v% solvent D (deionized distilled water 20%, acetonitrile 80%, TFA 0.1%). The flow rate of mobile phase was 1.0 mL/min, and the column effluent was monitored by UV/Vis detector at 245 nm for PHE and 254 nm for the other drugs at room temperature.

Pharmacokinetic analysis

Standard methods were used to calculate the following pharmacokinetic parameters using a non-compartmental analysis (WinNonlin, version 3.1,

NCA200 and 201; Pharsight Corporation, Mountain View, CA): the total area under the plasma concentration–time curve from time zero to time infinity (AUC); the time-averaged total body clearance (CL); the terminal half-life ($t_{1/2}$); the apparent volume of distribution at steady-state (Vss). The extent of absolute oral bioavailability (F; expressed as percent of dose administered) was calculated by dividing the dose-normalized AUC after oral administration by the dose-normalized AUC after intravenous injection. The peak plasma concentration (C_{max}) and time to reach C_{max} (T_{max}) were directly read from the experimental data.

Statistical analysis

A *p*-value less than 0.05 was considered to be statistically significant using a *t*-test between the two means for the unpaired data or a Duncan's multiple range test a *posteriori* ANOVA among the three means for the unpaired data. All results were expressed as mean ± standard deviation except median (ranges) for T_{max}.

1.4. RESULTS

In vitro CYP inhibition study in HLM and RLM

The effect of PU on *in vitro* metabolic reactions of the model CYP substrates in HLM (Fig. **2**) and RLM (Fig. **3**) was evaluated. As shown in Fig. **2**, the rate of disappearance of TES in HLM was significantly reduced in the presence of 10-μM PU by 28.2%. However, the rates of disappearance of PHE, DIC and DEX in HLM were not significantly changed by PU. The changes in the rates of disappearance of the model CYP substrates in RLM by PU were consistent with those in HLM. As shown in Fig. **3**, the rate of disappearance of TES in RLM was significantly reduced in presence of PU by 26.1%. However, the rates of disappearance of PHE, DIC and DEX in RLM were not significantly changed by PU. The dose–response curve for the inhibition of metabolic reaction of TES in the presence of PU in RLM was shown in Fig. **4**. A sigmoidal Hill equation was well fitted to the data (R^2 = 0.893–0.986). The IC_{50} and Hill coefficient of PU for the inhibition of metabolic reaction of TES was 15.5 ± 3.9 μM and 0.960 ± 0.074, respectively.

To evaluate the CYP-mediated metabolism of PU itself, the remaining fraction of PU (5, 10, 20, and 50 μM) after 0-min and 60-min incubation in RLM were determined in RLM (Fig. **5**). However, the remaining fractions of PU after

60-min incubation were not significantly different from those of control group (0-min incubation) at all PU concentrations, indicating the negligible CYP-mediated metabolism of PU in RLM.

***In vivo* pharmacokinetic study of BUS in rats**

BUS is known to be a probe substrate for human CYP3A4 (Ohno, Hisaka et al. 2007; Foti, Rock et al. 2010) and rat CYP3A (Rioux, Bellavance et al. 2013; Zhu, Yang et al. 2013), and it has been used as a CYP3A substrate in previous *in vivo* rat studies (Rioux, Bellavance et al. 2013; Zhu, Yang et al. 2013). Thus, BUS was selected as a substrate for the present *in vivo* rat study. The plasma concentration–time profiles of BUS after its intravenous administration at a dose of 10 mg/kg with or without 10-mg/kg intravenous PU in rats are shown in Fig. **6**, and relevant pharmacokinetic parameters are listed in Table **1**. Compared with control rats, the AUC and CL of intravenous BUS were significantly increased and decreased, respectively, by 1.61-fold, and the Vss of BUS was significantly decreased by 1.95-fold, while the $t_{1/2}$ of BUS was not significantly changed in rats treated with single simultaneous co-administration of intravenous PU (Table **1**). The plasma concentration–time profiles of BUS after its oral administration at a dose of 30 mg/kg with or without 10-mg/kg intravenous PU in rats are shown in Fig. **7**, and relevant pharmacokinetic parameters are listed in Table **2**. The

AUC and F of orally administered BUS were significantly increased by 1.51-fold in rats treated with single simultaneous co-administration of intravenous PU (Table **2**).

In vivo pharmacokinetic study of PU in rats

The plasma concentration–time profiles of PU after its intravenous injection at a dose of 10 mg/kg with 10-mg/kg intravenous BUS or 30-mg/kg oral BUS in rats are shown in Fig. **8**, and relevant pharmacokinetic parameters are listed in Table **3**. As shown in Fig. **8**, the *in vivo* plasma levels of PU were higher than 10 μM (4.16 μg/mL) during 30 min after its intravenous injection. The AUC, CL, Vss, and $t_{1/2}$ of intravenous PU in rats treated with single simultaneous co-administration of intravenous BUS were comparable with those in rats treated with single simultaneous co-administration of oral BUS (Table **3**).

1.5. DISCUSSION

The effect of PU on *in vitro* hepatic CYP-mediated metabolic activity in HLM and RLM was evaluated by the CYP inhibition study in the presence of PU at a concentration of 10 μM. The model CYP substrates and their concentrations (approximately equal to their K_m values) were as follows: PHE for CYP1A2 (10 μM), DIC for CYP2C9 (5 μM), DEX for CYP2D6 (5 μM), and TES for CYP3A4 (30 μM), which were selected based on previous studies (Leemann, Transon et al. 1993; Tassaneeyakul, Birkett et al. 1993; Transon, Leemann et al. 1996; Eagling, Tjia et al. 1998; Zhao, Ding et al. 2012). The results shown in Figs. **2** and **3** suggest that 10-μM PU may function as a direct inhibitor of human CYP3A4 and rat CYP3A1/2, reducing hepatic CYP3A-mediated metabolism in rats and human, while it may have no significant effect on CYP1A, 2C and 2D-mediated metabolism in rats and human. Moreover, the species similarities in CYP-modulating effects of PU between rats and human were observed. The Hill coefficients for the inhibitory effect of PU on the CYP3A-mediated metabolism of TES were close to 1, which is expected for competitive inhibition (Knutter, Kottra et al. 2009). Moreover, the results shown in Fig. **5** suggest that the CYP-mediated metabolism of PU may be negligible in RLM. Thus, it is plausible that PU inhibits CYP3A-mediated metabolism in a competitive manner but is not metabolized by CYPs. A previous study reported the direct inhibitory effect of

PU on aminopyrine demethylase (an indicator of CYP 1A, 2A, 2B, 2D, and 3A activity) in RLM (Guerra, Speroni et al. 2000; Hari Kumar and Kuttan 2006). However, the current results have first shown the inhibitory effect and its mechanism of PU on *in vitro* CYP3A-mediated metabolic activity in HLM or RLM.

To investigate the inhibitory effect of PU on the *in vivo* hepatic CYP3A-mediated metabolism, the pharmacokinetics of intravenous or oral BUS with or without single simultaneous co-administration of intravenous PU was evaluated in the rat model. Considering that intravenous BUS is known to be eliminated primarily *via* the hepatic metabolism in rats and human (Gammans, Mayol et al. 1986; Mahmood and Sahajwalla 1999), the significant decrease in the CL of BUS (Table **1**) could suggest reduction of hepatic clearance (CL_H) of BUS in rats with the 10-mg/kg intravenous PU administration. The CL_H of a drug depends on the hepatic blood flow (Q), protein binding in blood ($f_{u,B}$) and hepatic intrinsic clearance ($CL_{int,H}$) (Yoon, Han et al. 2012). Based on the results of the *in vitro* CYP inhibition study using RLM (Figs. **3** and **4**), it is plausible that 10-μM PU may reduce the $CL_{int,H}$ of CYP3A1/2 substrates including BUS in rats. Although the hepatic extraction ratio of BUS in rats has not been reported yet, the reduced CL of BUS in rats treated with single simultaneous co-administration of intravenous PU may at least be partly attributed to the direct inhibitory effect of

PU on the CYP3A1/2-mediated $CL_{int,H}$ of BUS. However, further investigation on the hepatic disposition of BUS and PU in rats is required to clarify the exact mechanism of the reduced CL of BUS by PU. The oral F of BUS in rats was 8.6% (Table **2**), which was in a good agreement with a reported human F value (approximately 5%) (Mahmood and Sahajwalla 1999). Although the exact reasons for the low F of BUS in rats and human have not been clarified yet, a previous *in-silico* study predicted that orally administered BUS might undergo an extensive hepatic first-pass metabolism in human (Obach, Walsky et al. 2006). Thus, the enhanced oral AUC and F of BUS in rats treated with single simultaneous co-administration of intravenous PU may attribute to the direct inhibitory effect of PU on the CYP3A1/2-mediated hepatic first-pass metabolism of oral BUS (Fig. **7** and Table **2**).

To confirm whether the intravenous PU dose (10 mg/kg) is sufficient for the inhibition of *in vivo* CYP3A1/2-mediated metabolism of BUS in rats, the pharmacokinetics of PU with single simultaneous co-administration of 10-mg/kg intravenous BUS or 30-mg/kg oral BUS in rats was evaluated. The PU dose was selected based on the clinical dosing mode of PU, *i.e.* intravenous injection at doses of 400–600 mg (6.67–10 mg/kg in 60-kg human) (Wang, Wu et al. 2006), and previous rat PK studies of intravenous PU (9–32 mg/kg) (Jin and Zhu 1992; Yan, Wang et al. 2006). The plasma levels of 10-mg/kg intravenous PU exceeded

the IC_{50} value of PU during the initial 30 mins (Fig. **8**). Since the distribution coefficient of PU in the rat liver is currently unknown, the PU concentration in the rat liver is difficult to be predicted from the plasma PU concentration data. Thus, assuming that the plasma concentration of PU can directly reflect the PU concentration in the rat liver (hepatocytes), it is plausible that 10-mg/kg intravenous PU could inhibit *in vivo* hepatic CYP3A-mediated drug metabolism in rats. As a result, the hepatic CYP3A-mediated metabolism of BUS was significantly reduced with 10-mg/kg intravenous PU (Figs. **6** and **7**), which confirmed that the selected PU dose was suitable for the present *in vivo* rat study. However, to evaluate dose-dependency for the inhibitory effect of PU on rat CYP3A activity, further investigation using higher PU doses may be required.

To the best of our knowledge, this is the first reported inhibitory effect of PU on *in vitro* CYP3A-mediated metabolic activity in HLM or RLM and *in vivo* hepatic CYP3A-mediated metabolism in rats. Therefore, this study would provide a good basis for predicting CYP3A-mediated herb–drug interactions.

1.6. CONCLUSIONS

The effect of PU on hepatic CYP-mediated drug metabolism in rats and human was investigated through an *in vitro* CYP inhibition study using HLM and RLM and *in vivo* pharmacokinetic study using rat model. The significant decrease in the rate of *in vitro* microsomal disappearance of TES together with the *in vivo* studies showing changes in pharmacokinetic parameters of BUS suggest that PU inhibits hepatic CYP3A-mediated drug metabolism. These results could lead to further studies in clinically significant metabolism-mediated herb–drug interactions.

References

Bardia, A., N. L. Nisly, et al. (2007). "Use of herbs among adults based on evidence-based indications: findings from the National Health Interview Survey." Mayo Clin Proc **82**(5): 561-566.

Bent, S. (2008). "Herbal medicine in the United States: review of efficacy, safety, and regulation: grand rounds at University of California, San Francisco Medical Center." J Gen Intern Med **23**(6): 854-859.

Eagling, V. A., J. F. Tjia, et al. (1998). "Differential selectivity of cytochrome P450 inhibitors against probe substrates in human and rat liver microsomes." Br J Clin Pharmacol **45**(2): 107-114.

Foti, R. S., D. A. Rock, et al. (2010). "Selection of alternative CYP3A4 probe substrates for clinical drug interaction studies using in vitro data and in vivo simulation." Drug Metab Dispos **38**(6): 981-987.

Gammans, R. E., R. F. Mayol, et al. (1986). "Metabolism and disposition of buspirone." Am J Med **80**(3B): 41-51.

Girennavar, B., G. K. Jayaprakasha, et al. (2007). "Potent inhibition of human cytochrome P450 3A4, 2D6, and 2C9 isoenzymes by grapefruit juice and its furocoumarins." J Food Sci **72**(8): C417-421.

Guerra, M. C., E. Speroni, et al. (2000). "Comparison between chinese medical

herb Pueraria lobata crude extract and its main isoflavone puerarin antioxidant properties and effects on rat liver CYP-catalysed drug metabolism." Life Sci **67**(24): 2997-3006.

Hari Kumar, K. B. and R. Kuttan (2006). "Inhibition of drug metabolizing enzymes (cytochrome P450) in vitro as well as in vivo by Phyllanthus amarus SCHUM & THONN." Biol Pharm Bull **29**(7): 1310-1313.

Jin, X. L. and X. Y. Zhu (1992). "Pharmacokinetics of puerarin in rats, rabbits, and dogs." Zhongguo Yao Li Xue Bao **13**(3): 284-288.

Jurica, J., J. Konecny, et al. (2010). "Simultaneous HPLC determination of tolbutamide, phenacetin and their metabolites as markers of cytochromes 1A2 and 2C6/11 in rat liver perfusate." J Pharm Biomed Anal **52**(4): 557-564.

Kennedy, D. A. and D. Seely (2010). "Clinically based evidence of drug-herb interactions: a systematic review." Expert Opin Drug Saf **9**(1): 79-124.

Kim, J. E., H. J. Cho, et al. (2013). "The limited intestinal absorption via paracellular pathway is responsible for the low oral bioavailability of doxorubicin." Xenobiotica **43**(7): 579-591.

Knutter, I., G. Kottra, et al. (2009). "High-affinity interaction of sartans with H+/peptide transporters." Drug Metab Dispos **37**(1): 143-149.

Komoroski, B. J., S. Zhang, et al. (2004). "Induction and inhibition of cytochromes P450 by the St. John's wort constituent hyperforin in human

hepatocyte cultures." Drug Metab Dispos **32**(5): 512-518.

Leemann, T., C. Transon, et al. (1993). "Cytochrome P450TB (CYP2C): a major monooxygenase catalyzing diclofenac 4'-hydroxylation in human liver." Life Sci **52**(1): 29-34.

Luo, C. F., B. Cai, et al. (2012). "UDP-glucuronosyltransferase 1A1 is the principal enzyme responsible for puerarin metabolism in human liver microsomes." Arch Toxicol **86**(11): 1681-1690.

Mahmood, I. and C. Sahajwalla (1999). "Clinical pharmacokinetics and pharmacodynamics of buspirone, an anxiolytic drug." Clin Pharmacokinet **36**(4): 277-287.

Mason, P. (2010). "Important drug-nutrient interactions." Proc Nutr Soc **69**(4): 551-557.

Mohamed, M. F. and R. F. Frye (2010). "Inhibition of intestinal and hepatic glucuronidation of mycophenolic acid by Ginkgo biloba extract and flavonoids." Drug Metab Dispos **38**(2): 270-275.

Obach, R. S., R. L. Walsky, et al. (2006). "The utility of in vitro cytochrome P450 inhibition data in the prediction of drug-drug interactions." J Pharmacol Exp Ther **316**(1): 336-348.

Ohno, Y., A. Hisaka, et al. (2007). "General framework for the quantitative prediction of CYP3A4-mediated oral drug interactions based on the AUC

increase by coadministration of standard drugs." Clin Pharmacokinet **46**(8): 681-696.

Rendic, S. (2002). "Summary of information on human CYP enzymes: human P450 metabolism data." Drug Metab Rev **34**(1-2): 83-448.

Reyes-Gordillo, K., P. Muriel, et al. (2007). "Pharmacokinetics of diclofenac in rats intoxicated with CCL4, and in the regenerating liver." Biopharm Drug Dispos **28**(8): 415-422.

Rioux, N., E. Bellavance, et al. (2013). "Assessment of CYP3A-mediated drug-drug interaction potential for victim drugs using an in vivo rat model." Biopharm Drug Dispos **34**(7): 396-401.

Tassaneeyakul, W., D. J. Birkett, et al. (1993). "Specificity of substrate and inhibitor probes for human cytochromes P450 1A1 and 1A2." J Pharmacol Exp Ther **265**(1): 401-407.

Tassaneeyakul, W., L. Q. Guo, et al. (2000). "Inhibition selectivity of grapefruit juice components on human cytochromes P450." Arch Biochem Biophys **378**(2): 356-363.

Transon, C., T. Leemann, et al. (1996). "In vitro comparative inhibition profiles of major human drug metabolising cytochrome P450 isozymes (CYP2C9, CYP2D6 and CYP3A4) by HMG-CoA reductase inhibitors." Eur J Clin Pharmacol **50**(3): 209-215.

Wang, Q., T. Wu, et al. (2006). "Puerarin injection for unstable angina pectoris." Cochrane Database Syst Rev **3**: CD004196.

Yan, B., W. Wang, et al. (2006). "Determination of puerarin in rat cortex by high-performance liquid chromatography after intravenous administration of Puerariae flavonoids." Biomed Chromatogr **20**(2): 180-184.

Yin, O. Q., B. Tomlinson, et al. (2004). "Pharmacogenetics and herb-drug interactions: experience with Ginkgo biloba and omeprazole." Pharmacogenetics **14**(12): 841-850.

Yoon, I., S. Han, et al. (2012). "Saturable sinusoidal uptake is rate-determining process in hepatic elimination of docetaxel in rats." Xenobiotica **42**(11): 1110-1119.

Zhang, R., C. Liu, et al. (2008). "Determination of cytochrome P450 3A4 activity with testosterone probe using high performance liquid chromatography." Se Pu **26**(1): 80-83.

Zhao, K., M. Ding, et al. (2012). "In-vitro metabolism of glycyrrhetinic acid by human and rat liver microsomes and its interactions with six CYP substrates." J Pharm Pharmacol **64**(10): 1445-1451.

Zheng, J., B. Chen, et al. (2010). "The effects of puerarin on CYP2D6 and CYP1A2 activities in vivo." Arch Pharm Res **33**(2): 243-246.

Zhou, S., Y. Gao, et al. (2003). "Interactions of herbs with cytochrome P450."

Drug Metab Rev **35**(1): 35-98.

Zhu, L., X. Yang, et al. (2013). "The exposure of highly toxic aconitine does not significantly impact the activity and expression of cytochrome P450 3A in rats determined by a novel ultra performance liquid chromatography-tandem mass spectrometric method of a specific probe buspirone." Food Chem Toxicol **51**: 396-403.

Table 1. Pharmacokinetic Parameters of BUS after Its Intravenous Injection at a Dose of 10 mg/kg Without or With 10-mg/kg Intravenous PU in Rats (n = 3).

Parameter	Control	+ PU
AUC (μg·min/mL)	132 ± 17.5	212 ± 26.2*
CL (mL/min/kg)	76.7 ± 9.93	47.6 ± 5.80*
Vss (mL/kg)	3570 ± 627	1830 ± 595*
$t_{1/2}$ (min)	42.2 ± 1.90	36.4 ± 5.95

* Significantly different from the Control group ($p < 0.05$).

Table 2. Pharmacokinetic Parameters of BUS after Its Oral Administration at a Dose of 30 mg/kg Without or With 10-mg/kg Intravenous PU in Rats (n = 3).

Parameter	Control	+ PU
AUC (μg·min/mL)	20.8 ± 4.06	43.3 ± 12.2*
C_{max} (μg/mL)	0.862 ± 0.601	1.88 ± 0.464
T_{max} (min)	5 (5–10)	5 (5–10)
F (%)	5.25	10.9

* Significantly different from the Control group ($p < 0.05$).

Table 3. Pharmacokinetic Parameters of PU after Its Intravenous Injection at a Dose of 10 mg/kg With 10-mg/kg Intravenous BUS (+ IV-BUS) or 30-mg/kg Oral BUS (+ PO-BUS) in Rats (*n* = 3).

Parameter	+ IV-BUS	+ PO-BUS
AUC (μg·min/mL)	687 ± 214	755 ± 183
CL (mL/min/kg)	15.5 ± 4.54	13.9 ± 3.91
Vss (mL/kg)	250 ± 90.5	261 ± 75.6
$t_{1/2}$ (min)	17.8 ± 3.34	16.3 ± 4.82

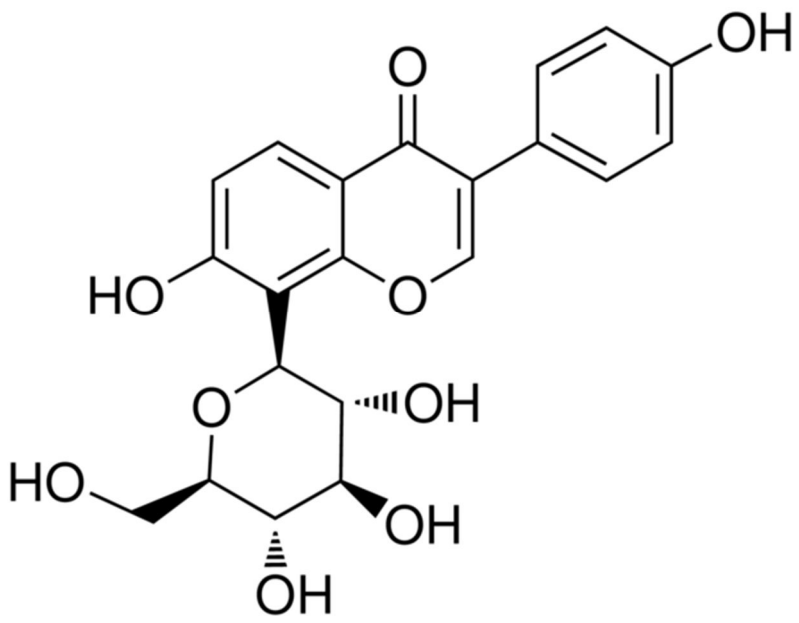

Figure 1. Chemical Structure of PU.

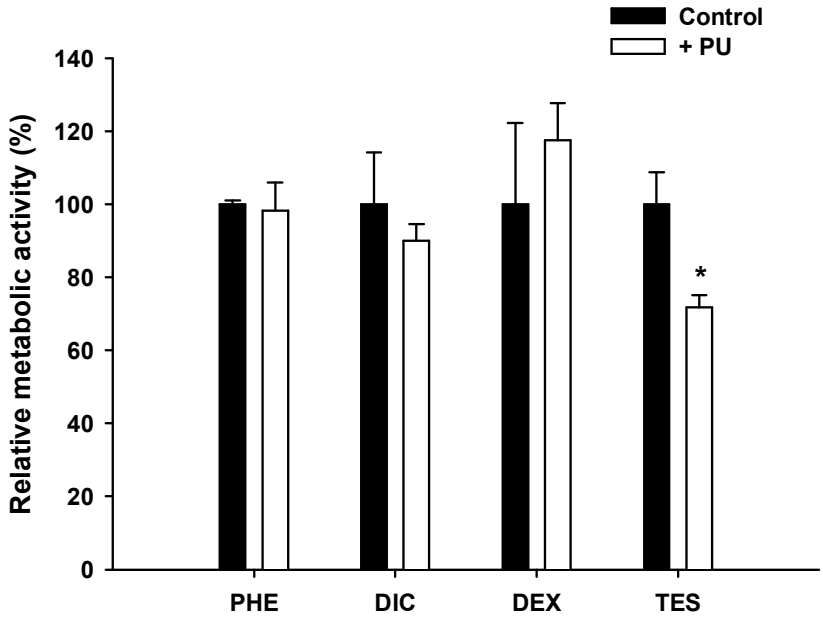

Figure 2. Effect of PU on Metabolic Reactions of Model CYP Substrates (PHE, Phenacetin; DIC, Diclofenac; DEX, Dextromethorphan; TES, Testosterone) in HLM (n = 3). *, Significantly different from the control group ($p < 0.05$).

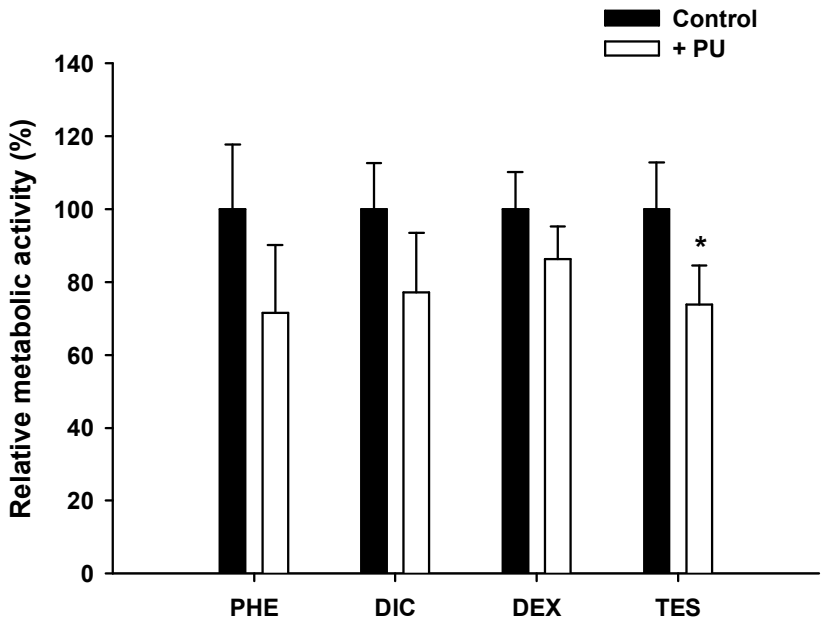

Figure 3. Effect of PU on Metabolic Reactions of Model CYP Substrates (PHE, Phenacetin; DIC, Diclofenac; DEX, Dextromethorphan; TES, Testosterone) in RLM (n = 3). *, Significantly different from the control group ($p < 0.05$).

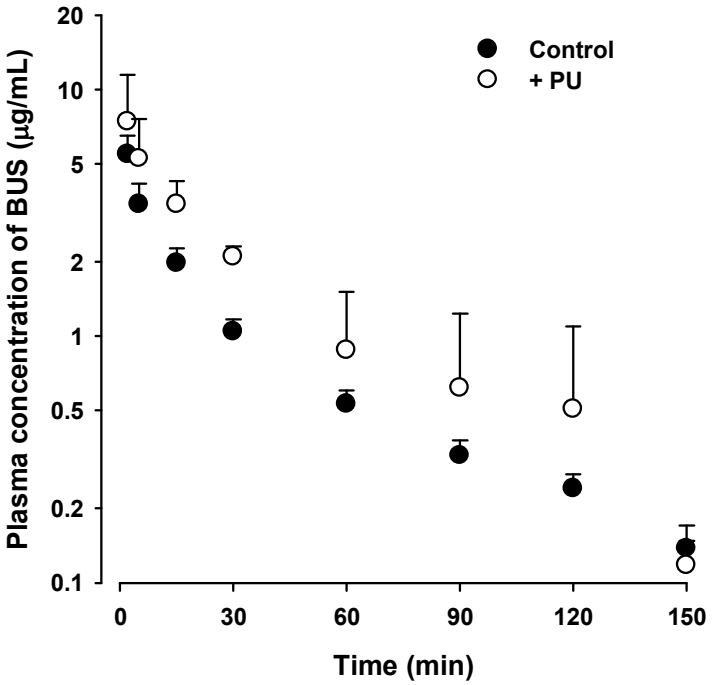

Figure 4. Plasma Concentration–Time Profiles of BUS after Its Intravenous Injection at a Dose of 10 mg/kg Without (●) or With (○) 10-mg/kg Intravenous PU in Rats (n = 3).

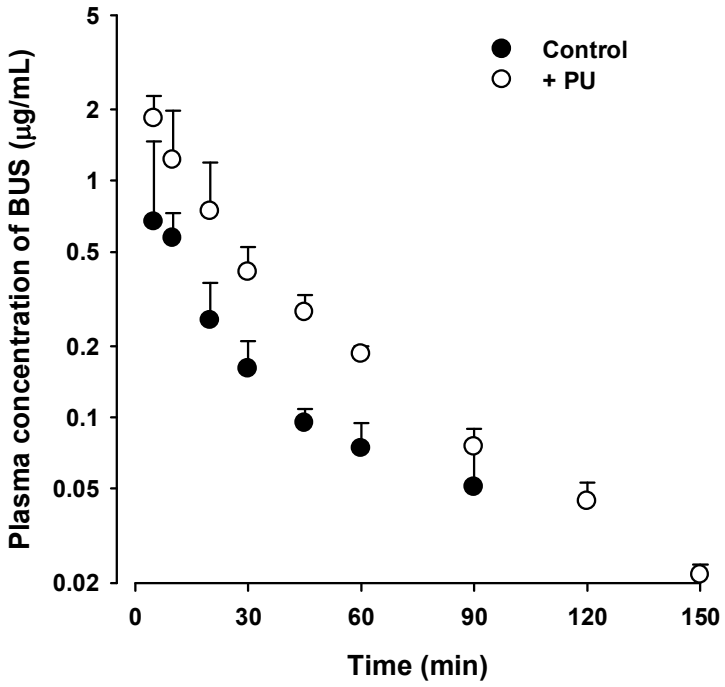

Figure 5. Plasma Concentration–Time Profiles of BUS after Its Oral Administration at a Dose of 30 mg/kg Without (●) or With (○) 10-mg/kg Intravenous PU in Rats (n = 3).

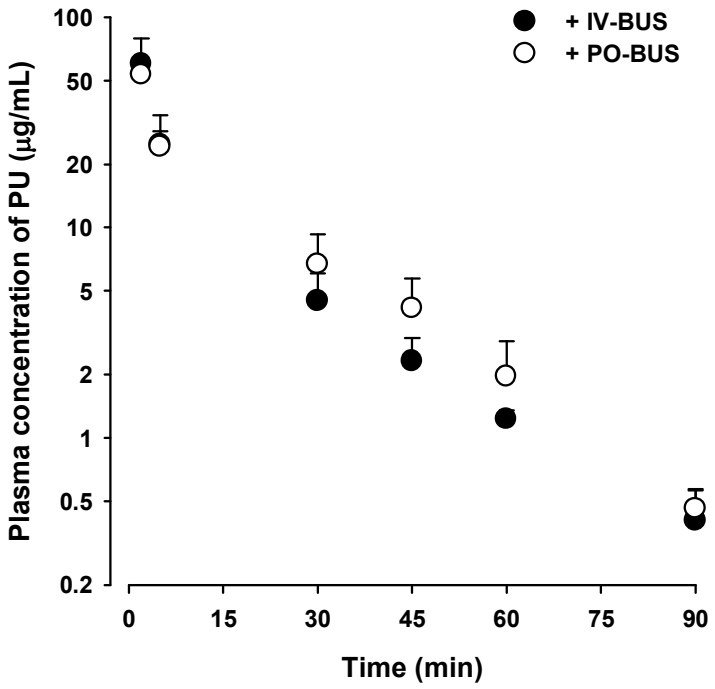

Figure 6. Plasma Concentration–Time Profiles of PU after Its Intravenous Injection at a Dose of 10 mg/kg With 10-mg/kg Intravenous BUS (●, + IV-BUS) or 30-mg/kg Oral BUS (○, + PO-BUS) in Rats (n = 3).

Part II

Metabolic interactions of magnolol with cytochrome P450 enzymes in human and rat liver microsomes

2.1. ABSTRACT

Magnolol (MAG; 5,5'-Diallyl-2,2'-biphenyldiol) is a major bioactive component of *Magnolia officinalis*. The metabolic interactions of MAG with hepatic cytochrome P450 monooxygenase (CYP) through *in vitro* microsomal metabolism study using human and rat liver microsomes (HLM and RLM, respectively) was investigated. In HLM and RLM, CYP2C and 3A subfamilies were significantly involved in the metabolism of MAG, while CYP1A subfamily was not. The relative contribution of phase I enzymes including CYP to the metabolism of MAG was comparable to that of uridine diphosphate glucuronosyltransferase (UGT) in RLM. Moreover, MAG potently inhibited the metabolic activity of CYP1A and 2C subfamilies, while weakly CYP3A subfamily in HLM and RLM. Based on Dixon plot, the inhibition type of MAG on CYP activity in RLM was determined as follows: uncompetitive inhibitor for CYP1A; competitive inhibitor for CYP2C and 3A. These results could lead to further studies in clinically significant metabolism-mediated MAG–drug interactions.

Keywords: Magnolol, Cytochrome P450, Rat liver microsomes, Human liver microsomes, Metabolism

Abbreviations: MAG, magnolol; CYP, cytochrome P450 monooxygenase; UGT, uridine diphosphate glucuronosyltransferase; HLM, human liver microsomes; RLM, rat liver microsomes; DIC, diclofenac; KCZ, ketoconazole; NF, α-naphtoflavone; PHE, phenacetin; SPZ, sulfaphenazole; TES, testosterone; UDPGA, uridine-5-diphospho-glucuronic acid trisodium salt; V_{max}, maximal metabolic rate; K_m, Michaelis–Menten constant; CL_{int}, intrinsic metabolic clearance.

2.2. INTRODUCTION

Herbal medicines are widely used for the prevention and treatment of common illnesses (Chang, 2000). However, some herbal extracts and phytochemicals have been reported to modulate drug metabolizing enzyme activity, leading to herb–drug interactions which may cause adverse reactions such as toxicity and therapeutic failure (Zhang *et al.*, 2011; Kennedy and Seely, 2010). Among the various drug metabolizing enzymes, cytochrome P450 monooxygenase (CYP) is typically involved in clinically significant interactions between prescribed drugs and herbs (Jeong *et al.*, 2013). Grapefruit (*Citrus paradisi*), St. John's wort (*Hypericum perforatum*), ginkgo (*Ginkgo biloba*), and licolice (*Glycyrrhiza glabra*) have all been reported to alter the CYP-mediated metabolism and efficacy of anticoagulants, anticancer drugs, antiretroviral drugs, antihyperlipidemic drugs, immunosuppressants, and/or antidepressants (Chen *et al.*, 2011; He *et al.*, 2010; Mason, 2010; Borrelli and Izzo, 2009). Therefore, examining the CYP-mediated herb–drug interactions and their mechanisms in animals and human could be a good basis for the optimal design of drug and herb-based therapies.

Magnolol (MAG; 5,5'-Diallyl-2,2'-biphenyldiol; Fig. 1) is a major bioactive component of *Magnolia officinalis* (Joo and Liu, 2013). MAG has been reported

to possess anticancer, antibacterial, antioxidative, and anti-inflammatory activities (Zhu *et al.*, 2012a; Chen *et al.*, 2009; Lee *et al.*, 2009; Park *et al.*, 2004). *Magnolia officinalis* is currently used as a herbal medicine for the treatment of nervous disturbance, abdominal disorders, gastrointestinal food stagnancy, abdominal distention, constipation, coughing, and dyspnea (Zhu *et al.*, 2012b). Moreover, human could be significantly exposed to MAG in daily life, because magnolia bark supercritical carbon dioxide extract (containing more than 92.5-% MAG) is added to mints and chewing gums to remove oral malodor (Greenberg *et al.*, 2007). It has been reported that teenage exposure to MAG can reach 1.64 mg/kg per day (Zhu *et al.*, 2012b).

To date, only a few studies have reported the inhibitory effect of MAG on CYP (IC_{50} values) and uridine diphosphate glucuronosyltransferase (UGT) (K_i values and inhibition types) activities in human liver microsomes (HLM) and/or recombinant UGT (Joo and Liu, 2013; Zhu *et al.*, 2012a). Moreover, it has been reported that MAG is metabolized by multiple UGT isoforms in HLM (Zhu *et al.*, 2012b). However, little information is available regarding the CYP-mediated metabolism of MAG and the inhibition type of MAG on CYP activity in HLM and rat liver microsomes (RLM). Therefore, further investigation on these issues is required for the improved understanding of CYP-mediated MAG–drug interactions. Herein, the metabolic interactions of MAG with CYP in HLM and

RLM were examined. CYP isoforms involved in the metabolism of MAG were identified, and the relative contribution of CYP and UGT to the metabolism of MAG was investigated in HLM and/or RLM. Then, the inhibitory effect of MAG on CYP activity in HLM and/or RLM was evaluated for its inhibition constants (IC_{50} and K_i) and inhibition types.

2.3. MATERIALS AND METHODS

Materials

Alamethicin, diclofenac (DIC), ketoconazole (KCZ), MAG, α-naphtoflavone (NF), phenacetin (PHE), sulfaphenazole (SPZ), testosterone (TES), and uridine-5-diphospho-glucuronic acid trisodium salt (UDPGA) were purchased from Sigma–Aldrich (St. Louis, MO, USA). BD-UltraPool^{TM} HLM 150 (150-donor pool) and nicotinamide adenine dinucleotide phosphate (NADPH) regenerating system were purchased from BD-Genetech (Woburn, MA, USA). Other chemicals were of reagent grade or high-performance liquid chromatography (HPLC) grade.

Animals

Protocols for the animal studies were approved by the Institutional Animal Care and Use Committee of Seoul National University (Seoul, Korea). Male SD rats (7–9 weeks old and weighing 200–250 g) were purchased from Orient Bio, Inc. (Seongnam, Korea). They were maintained in a clean room (Animal Center for Pharmaceutical Research, College of Pharmacy, Seoul National University) at a temperature of 20–23°C with 12-h light (07:00–19:00) and dark (19:00–07:00) cycles, and a relative humidity of 50 ± 5%. The rats were housed in metabolic

cages (Tecniplast, Varese, Italy) under filtered, pathogen-free air, with food (Agribrands Purina, Korea; Pyeongtaek, Korea) and water available *ad libitum*.

Preparation of RLM

RLM were prepared using a reported method (Yoon *et al.*, 2011). In brief, the livers of overnight fasted rats were homogenized using a 15-mL Pyrex glass homogenizer (Ultra-Turrax T25; Janke and Kunkel, IKALabortechnik, Staufeni, Germany) in ice-cold buffer of 0.154 M KCl/50 mM Tris–HCl in 1 mM EDTA (pH 7.4). The homogenate was centrifuged (16,000 *g*, 30 min) and the supernatant fraction was further centrifuged (100,000 *g*, 90 min). The microsomal pellet was resuspended in the buffer of 0.154 M KCl/50 mM Tris–HCl in 1 mM EDTA (pH 7.4). The microsomal preparations were stored at –70^{o}C until use.

CYP-mediated metabolism of MAG in HLM and RLM

To evaluate the CYP-mediated metabolism of MAG, the disappearance of MAG in the absence or presence of specific CYP isoform-selective inhibitors was determined in HLM and RLM. Microsomal incubation mixtures were prepared in a total volume of 500 μL as follows: HLM or RLM (0.5-mg/mL microsomal protein), 1-mM NADPH, 10-mM $MgCl_2$, 50-mM potassium phosphate buffer,

MAG (10 μM), CYP isoform-selective inhibitors (1-μM NF for human CYP1A2 and rat CYP1A, 10-μM SPZ for human CYP2C9 and rat CYP2C, 10-μM KCZ for human CYP3A4 and rat CYP3A) (Khojasteh *et al.*, 2011; Bowalgaha *et al.*, 2005). At 0 and 20 min after starting the metabolic reaction, 100 μL of the incubation mixture was sampled and transferred into a clean 1.5-mL eppendorf tube containing 100-μL acetonitrile to terminate the metabolic reaction. After vortex-mixing and centrifugation at 16,000 *g* for 10 min, 100-μL aliquot of the supernatant was stored at –70°C freezer until HPLC analysis. To evaluate the relative contribution of CYP and UGT to the metabolism of MAG, the disappearance of MAG at various concentrations (4–200 μM) in the presence of either or both of NADPH and UDPGA/alamethicin was determined in RLM. The following Michaelis–Menten equation (Eq. 1) was simultaneously fit to the substrate (MAG) concentration ([S]; μM) versus initial metabolic rate (V; nmol/min/mg protein):

$$V = \frac{V_{max} \times [S]}{K_m + [S]} \quad (1)$$

where the V_{max} and K_m are the maximal metabolic rate and Michaelis–Menten constant, respectively. The intrinsic metabolic clearance (CL_{int}) was calculated as V_{max} / K_m.

Inhibitory effect of MAG on CYP activity in HLM and RLM

For *in vitro* CYP inhibition study, microsomal incubation mixtures were prepared in a total volume of 500 μL as follows: HLM or RLM (0.5-mg/mL microsomal protein), 1-mM NADPH, 10-mM $MgCl_2$, 50-mM potassium phosphate buffer, various concentrations of MAG (0.1–200 μM), CYP isoform-specific probe substrate (10-μM PHE for human CYP1A2 and rat CYP 1A, 5-μM DIC for human CYP2C9 and rat CYP2C, and 30-μM TES for human CYP3A4 and rat CYP3A) (Zhang *et al.*, 2013; Yeung and Or, 2012; Zhao *et al.*, 2012). Reactions were initiated by the addition of each CYP probe substrate, and incubations were carried out at 37^{o}C in a shaking water bath. At 0, 5, 10, and 30 min after starting the metabolic reaction, 100 μL of the incubation mixture was sampled and transferred into a clean 1.5-mL eppendorf tube containing 100-μL acetonitrile to terminate the metabolic reaction. After vortex-mixing and centrifugation at 16,000 *g* for 10 min, 100-μL aliquot of the supernatant was stored at –70^{o}C freezer until HPLC analysis.

HPLC analysis

The concentrations of MAG, PHE, DIC, and TES in the microsomal samples were determined as previously reported with slight modifications (Jurica *et al.*, 2010; Basha *et al.*, 2007; Sun *et al.*, 2003; Tsai *et al.*, 1994). The 100-μL samples

prepared as described above were directly injected into the HPLC column. The mobile phase was a mixture of 20-mM phosphate monobasic solution (PH 2.4, solvent A) and acetonitrile (solvent B). For PHE, the following gradient system was used: solvent A of 70 v/v% to 30 v/v% during 0–8 min; solvent A of 70 v/v% during 8–11 min. For DIC, the following gradient system was used: solvent A of 45 v/v% to 18 v/v% during 0–6 min; solvent A of 45 v/v% during 6–8 min. For TES, the mobile phase was composed of 50-v/v% solvent C (deionized distilled water 95%, acetonitrile 5%, TFA 0.1%) and 50-v/v% solvent D (deionized distilled water 20%, acetonitrile 80%, TFA 0.1%). For MAG, the following gradient system was used: solvent A of 45 v/v% to 15 v/v% during 0–6 min; solvent A of 45 v/v% during 6–8 min. The flow rate of mobile phase was 1.0 mL/min, and the column effluent was monitored by UV/Vis detector at 245 nm for PHE, 254 nm for DIC and TES, 280nm for MAG at room temperature.

Data analysis

The IC_{50} value of MAG for the inhibition of CYP activity was determined by nonlinear regression using GraphPad Prism 5.01 (GraphPad Software, San Diego, CA) according to Hill equation (Eq. 2):

$$y = \mathrm{Min} + \frac{\mathrm{Max} - \mathrm{Min}}{1 + (\frac{x}{IC_{50}})^{-P}} \quad (2)$$

where Max and Min are the initial and final y value, respectively, and the power P represents Hill coefficient. Control samples (with no inhibitor) were assayed in each analytical run. The inhibition type of MAG on CYP activity was determined graphically from Dixon plots, and the K_i value was calculated based on either competitive inhibition model (Eq. 3) or uncompetitive inhibition model (Eq. 4):

$$V = \frac{V_{max} \times [S]}{K_m\left(1 + \frac{[I]}{K_i}\right) + [S]} \quad (3)$$

$$V = \frac{\left(\frac{V_{max}}{1+\frac{[I]}{K_i}}\right) \times [S]}{\left(\frac{K_m}{1+\frac{[I]}{K_i}}\right) + [S]} \quad (4)$$

where V is the velocity of the reaction, and [S] and [I] are the substrate and inhibitor concentrations, respectively.

Statistical analysis

A *p*-value of less than 0.05 was considered to be statistically significant using a *t*-test between the two means for the unpaired data or a Duncan's multiple range test a *posteriori* analysis of variance (ANOVA) among the three means for the unpaired data. All data were rounded to three significant figures and expressed as mean ± standard deviation.

2.4. RESULTS

CYP-mediated metabolism of MAG in HLM and RLM

The effects of selective CYP inhibitors on the metabolic reaction of MAG in HLM and RLM were evaluated (Figs. 2 and 3). The disappearance of MAG was significantly reduced in the presence of SPZ and KCZ by 65.6 and 40.3% in HLM and 35.3 and 49.7% in RLM, while it was not affected by NF. Concentration dependency for the metabolic reaction of MAG in RLM in the presence of either or both of NADPH and UDPGA/alamethicin was shown in Fig. 4, and relevant kinetic parameters are listed in Table 1. In microsomal preparations, the monooxygenases (including CYP)-mediated oxidation (phase I metabolism) occurs in the presence of NADPH alone, while the UGT-mediated glucuronidation (phase II metabolism) in the presence of UDPGA and alamethicin (Fisher *et al.*, 2000). Thus, the metabolism of MAG in the 'NADPH' group was mediated primarily by the phase I enzymes including CYP, while that in the 'UDPGA/alamethicin' group was mediated exclusively by UGT. In the 'NADPH + UDPGA/alamethicin' group, the metabolism of MAG was mediated by both the phase I enzymes and UGT. The saturable and concentration-dependent kinetics observed in the three groups were successfully described by assuming the presence of one saturable component (Fig. 4). The V_{max} value of

the ‘NADPH’ group was significantly lower than that of the other groups, while the K_m value of the ‘UDPGA/alamethicin’ group was significantly higher than that of the ‘NADPH’ group (Table 1). There was no significant difference in the CL_{int} values among the three groups.

Inhibitory effect of MAG on CYP activity in HLM and RLM

The effects of MAG on the metabolic reaction of the model CYP substrates were evaluated in HLM (Fig. 5). The disappearance of PHE, DIC and TES was significantly reduced in presence of 10-μM MAG by 80.6, 72.9 and 29.5%, respectively, indicating the inhibitory effect of MAG on human CYP1A2, 2C9 and 3A4. The inhibitory effect of MAG on the disappearance of PHE, DIC and TES in RLM was in line with the results in HLM. The inhibition of CYP1A, 2C and 3A activities by MAG at various concentrations in RLM was well described by the sigmoidal Hill equation (Fig. 6), and the IC_{50} values of MAG for the inhibition of CYP activity in RLM are listed in Table 2. The inhibition type of MAG on CYP activity was further evaluated by the construction of Dixon plot (Fig. 7). The graphical analysis of Dixon plot indicated that MAG inhibited CYP1A activity *via* uncompetitive inhibition mechanism, while CYP2C and 3A activities *via* competitive inhibition mechanism. The K_i values estimated from relevant inhibition models (Eqs. 3 and 4) are listed in Table 2.

2.5. DISCUSSION

The CYP isoforms involved in the metabolism of MAG were identified by examining the disappearance of MAG in the presence of specific CYP isoform-selective inhibitor in HLM (Fig. 2) and RLM (Fig. 3). The result shown in Fig. 2 suggests that CYP2C9 and 3A4 are involved in the metabolism of MAG in human, while CYP1A2 is not. The result in RLM was consistent with that in HLM, suggesting that CYP2C and 3A are involved in the metabolism of MAG in rats, while CYP1A is not (Fig. 3). The CYP and/or UGT-mediated metabolism of MAG at various concentrations was further evaluated in RLM (Fig. 4 and Table 1). As shown in Table 1, the V_{max} and K_m values of the 'UPDGA/alamethicin' group were significantly higher than those of the 'NADPH' group, suggesting that UGT might have a higher capacity and lower affinity for the metabolism of MAG compared with phase I enzymes including CYP. Consequently, the CL_{int} value of the 'NADPH' group was comparable to that of the 'UDPGA/alamethicin' group. This result suggests that the phase I enzymes including CYP as well as UGT could significantly contribute to the metabolism of MAG.

In HLM, the inhibition potential of 10-μM MAG on CYP1A2 and 2C9 activities was markedly higher than that on CYP3A4 activity (Fig. 5), which is

consistent with recent previous study (Joo and Liu, 2013). Similarly, MAG potently inhibited the metabolic activity of CYP1A and 2C with IC_{50} values of 1.62 and 5.56 μM, respectively, while weakly CYP3A with a IC_{50} value of 35.0 μM in RLM (Fig. 6 and Table 2). In enzyme inhibition studies, the apparent K_i value could be a better parameter to describe the extent of interaction of an inhibitor with a particular enzyme (Jeong *et al.*, 2013). Thus, the K_i values and inhibition types of MAG on CYP-mediated metabolic activity in RLM were determined from Dixon plots, showing that MAG could function as a CYP inhibitor in the following manner: a potent and uncompetitive inhibitor for CYP1A; a potent and competitive inhibitor for CYP2C; a weak and competitive inhibitor for CYP3A.

To the best of our knowledge, this is the first report on the significant contribution of phase I enzymes including CYP to the metabolism of MAG and the inhibition type of MAG on CYP activity in HLM and/or RLM. Therefore, this study would provide a good basis for predicting CYP-mediated MAG–drug interactions.

2.6. CONCLUSIONS

The metabolic interactions of MAG with CYP were investigated through *in vitro* microsomal metabolism study. In HLM and RLM, CYP2C and 3A subfamilies were significantly involved in the metabolism of MAG, while CYP1A subfamily was not. The relative contribution of phase I enzymes including CYP to the metabolism of MAG was comparable to that of UGT in RLM. Moreover, MAG potently inhibited the metabolic activity of CYP1A and 2C subfamilies, while weakly CYP3A subfamily in HLM and RLM. Based on Dixon plot, the inhibition type of MAG on CYP activity in RLM was determined as follows: uncompetitive inhibitor for CYP1A; competitive inhibitor for CYP2C and 3A. These results could lead to further studies in clinically significant metabolism-mediated MAG–drug interactions.

2.7. REFERENCES

Basha SJ, Naveed SA, Tiwari NK, Shashikumar D, Muzeeb S, Kumar TR, Kumar NV, Rao NP, Srinivas N, Mullangi R, Srinivas NR. 2007. Concurrent determination of ezetimibe and its phase-I and II metabolites by HPLC with UV detection: quantitative application to various in vitro metabolic stability studies and for qualitative estimation in bile. J Chromatogr B Analyt Technol Biomed Life Sci, 853: 88-96.

Borrelli F, Izzo AA. 2009. Herb-drug interactions with St John's wort (Hypericum perforatum): an update on clinical observations. AAPS J, 11: 710-727.

Bowalgaha K, Elliot DJ, Mackenzie PI, Knights KM, Swedmark S, Miners JO. 2005. S-Naproxen and desmethylnaproxen glucuronidation by human liver microsomes and recombinant human UDP-glucuronosyltransferases (UGT): role of UGT2B7 in the elimination of naproxen. Br J Clin Pharmacol, 60: 423-433.

Chang J. 2000. Medicinal herbs: drugs or dietary supplements? Biochem Pharmacol, 59: 211-219.

Chen XW, Serag ES, Sneed KB, Liang J, Chew H, Pan SY, Zhou SF. 2011. Clinical herbal interactions with conventional drugs: from molecules to maladies. Curr Med Chem, 18: 4836-4850.

Chen YH, Lin FY, Liu PL, Huang YT, Chiu JH, Chang YC, Man KM, Hong CY, Ho YY, Lai MT. 2009. Antioxidative and hepatoprotective effects of magnolol on acetaminophen-induced liver damage in rats. Arch Pharm Res, 32: 221-228.

Fisher MB, Campanale K, Ackermann BL, VandenBranden M, Wrighton SA. 2000. In vitro glucuronidation using human liver microsomes and the pore-forming peptide alamethicin. Drug Metab Dispos, 28: 560-566.

Greenberg M, Urnezis P, Tian M. 2007. Compressed mints and chewing gum containing magnolia bark extract are effective against bacteria responsible for oral malodor. J Agric Food Chem, 55: 9465-9469.

He SM, Yang AK, Li XT, Du YM, Zhou SF. 2010. Effects of herbal products on the metabolism and transport of anticancer agents. Expert Opin Drug Metab Toxicol, 6: 1195-1213.

Jeong HU, Kong TY, Kwon SS, Hong SW, Yeon SH, Choi JH, Lee JY, Cho YY, Lee HS. 2013. Effect of honokiol on cytochrome P450 and UDP-glucuronosyltransferase enzyme activities in human liver microsomes. Molecules, 18: 10681-10693.

Joo J, Liu K-H. 2013. Inhibitory effect of honokiol and magnolol on cytochrome P450 enzyme activities in human liver microsomes. Mass Spectrometry Letters, 4: 34-37.

Jurica J, Konecny J, Zahradnikova LZ, Tomandl J. 2010. Simultaneous HPLC

determination of tolbutamide, phenacetin and their metabolites as markers of cytochromes 1A2 and 2C6/11 in rat liver perfusate. J Pharm Biomed Anal, 52: 557-564.

Kennedy DA, Seely D. 2010. Clinically based evidence of drug-herb interactions: a systematic review. Expert Opin Drug Saf, 9: 79-124.

Khojasteh SC, Prabhu S, Kenny JR, Halladay JS, Lu AY. 2011. Chemical inhibitors of cytochrome P450 isoforms in human liver microsomes: a re-evaluation of P450 isoform selectivity. Eur J Drug Metab Pharmacokinet, 36: 1-16.

Lee DH, Szczepanski MJ, Lee YJ. 2009. Magnolol induces apoptosis via inhibiting the EGFR/PI3K/Akt signaling pathway in human prostate cancer cells. J Cell Biochem, 106: 1113-1122.

Mason P. 2010. Important drug-nutrient interactions. Proc Nutr Soc, 69: 551-557.

Park J, Lee J, Jung E, Park Y, Kim K, Park B, Jung K, Park E, Kim J, Park D. 2004. In vitro antibacterial and anti-inflammatory effects of honokiol and magnolol against Propionibacterium sp. Eur J Pharmacol, 496: 189-195.

Sun Y, Takaba K, Kido H, Nakashima MN, Nakashima K. 2003. Simultaneous determination of arylpropionic acidic non-steroidal anti-inflammatory drugs in pharmaceutical formulations and human plasma by HPLC with UV detection. J Pharm Biomed Anal, 30: 1611-1619.

Tsai TH, Chou CJ, Chen CF. 1994. Disposition of magnolol after intravenous bolus and infusion in rabbits. Drug Metab Dispos, 22: 518-521.

Yeung JH, Or PM. 2012. Polysaccharide peptides from Coriolus versicolor competitively inhibit model cytochrome P450 enzyme probe substrates metabolism in human liver microsomes. Phytomedicine, 19: 457-463.

Yoon IS, Choi MK, Kim JS, Shim CK, Chung SJ, Kim DD. 2011. Pharmacokinetics and first-pass elimination of metoprolol in rats: contribution of intestinal first-pass extraction to low bioavailability of metoprolol. Xenobiotica, 41: 243-251.

Zhang YH, Zhang YJ, Guo YL, Li WJ, Yu C. 2013. Astragaloside IV inhibited the activity of CYP1A2 in liver microsomes and influenced theophylline pharmacokinetics in rats. J Pharm Pharmacol, 65: 149-155.

Zhang ZJ, Tan QR, Tong Y, Wang XY, Wang HH, Ho LM, Wong HK, Feng YB, Wang D, Ng R, McAlonan GM, Wang CY, Wong VT. 2011. An epidemiological study of concomitant use of Chinese medicine and antipsychotics in schizophrenic patients: implication for herb-drug interaction. PLoS One, 6: e17239.

Zhao K, Ding M, Cao H, Cao ZX. 2012. In-vitro metabolism of glycyrrhetinic acid by human and rat liver microsomes and its interactions with six CYP substrates. J Pharm Pharmacol, 64: 1445-1451.

Zhu L, Ge G, Liu Y, He G, Liang S, Fang Z, Dong P, Cao Y, Yang L. 2012a. Potent and selective inhibition of magnolol on catalytic activities of UGT1A7 and 1A9. Xenobiotica, 42: 1001-1008.

Zhu L, Ge G, Zhang H, Liu H, He G, Liang S, Zhang Y, Fang Z, Dong P, Finel M, Yang L. 2012b. Characterization of hepatic and intestinal glucuronidation of magnolol: application of the relative activity factor approach to decipher the contributions of multiple UDP-glucuronosyltransferase isoforms. Drug Metab Dispos, 40: 529-538.

Table 1. V_{max}, K_m and CL_{int} values for the disappearance of MAG at various concentrations in RLM in the presence of either or both of NADPH and UDPGA/alamethicin (n = 3).

Parameter	NADPH[a]	UDPGA/ alamethicin[b]	NADPH + UDPGA/ alamethicin[c]
V_{max} (nmol/min/mg protein)	1.03 ± 0.246[*]	2.96 ± 0.408	3.69 ± 1.05
K_m (μM)	11.1 ± 8.37	49.7 ± 16.7[#]	24.4 ± 13.5
CL_{int} (mL/min/mg protein)	0.123 ± 0.0640	0.0621 ± 0.0112	0.165 ± 0.0368

[*] Significantly different from the other groups ($p < 0.05$).

[#] Significantly different from the 'Control' group ($p < 0.05$).

[a] NADPH was added to the microsomal incubation mixture, while UDPGA and alamethicin were not.

[b] UDPGA and alamethicin were added to the microsomal incubation mixture, while NADPH was not.

[c] NADPH, UDPGA and alamethicin were added to the microsomal incubation mixture.

Table 2. Inhibition constants and inhibition types of MAG on CYP activities in RLM.

Enzyme	IC_{50} (μM)	K_i (μM)	Type of inhibition
CYP1A	1.62 ± 0.423	1.09–12.0	Uncompetitive
CYP2C	5.56 ± 2.87	10.0–15.2	Competitive
CYP3A	35.0 ± 12.7	93.7–183	Competitive

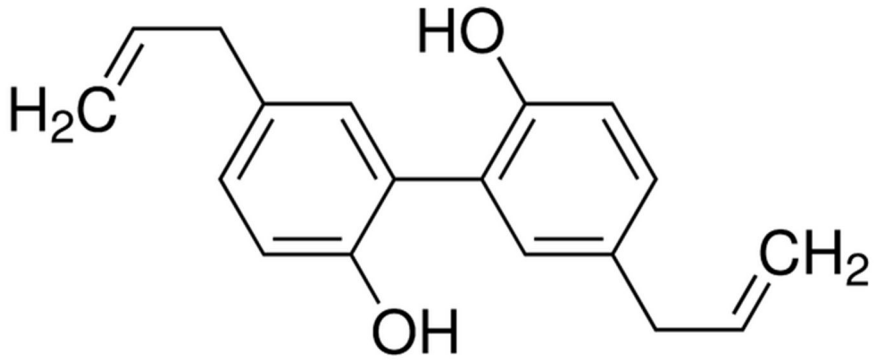

Figure 1. Chemical structure of MAG.

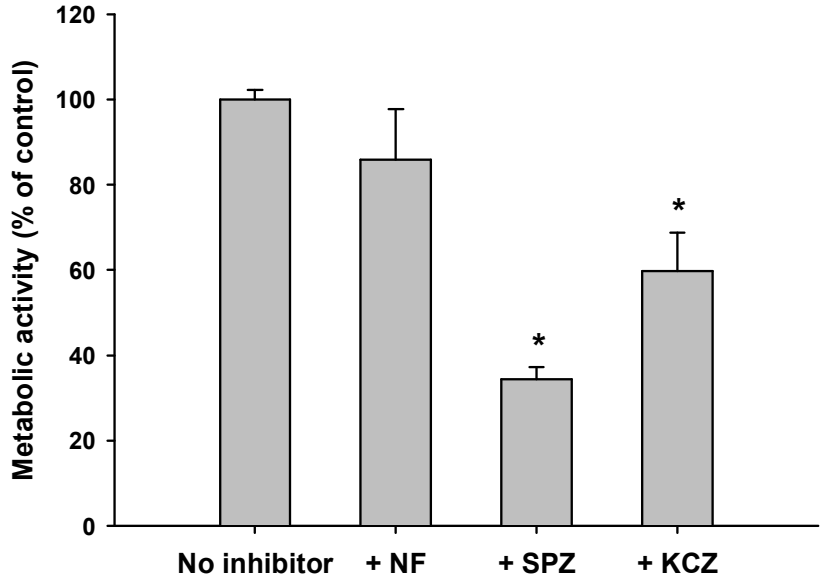

Figure 2. Effect of selective CYP inhibitors on the metabolic reaction of MAG in HLM ($n = 3$). *, significantly different from the control (no inhibitor) group ($p < 0.05$).

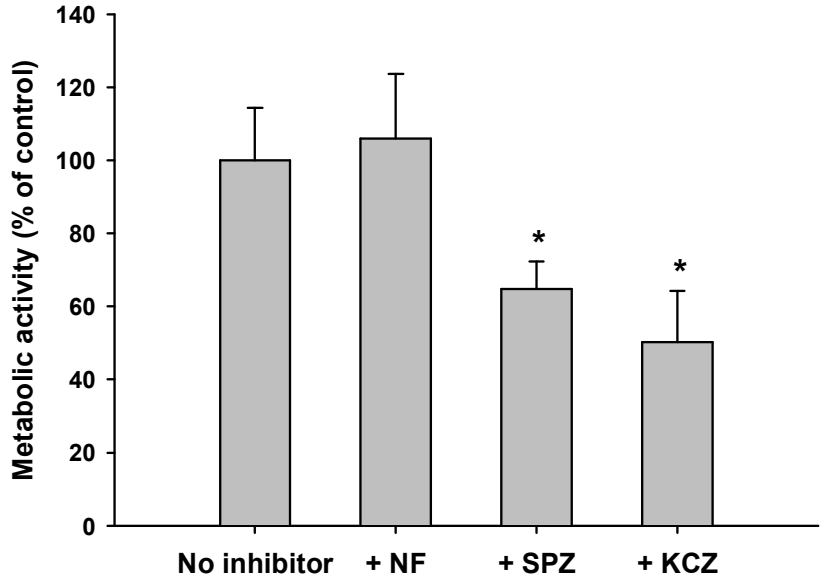

Figure 3. Effect of selective CYP inhibitors on the metabolic reaction of MAG in RLM ($n = 3$). *, significantly different from the control (no inhibitor) group ($p < 0.05$).

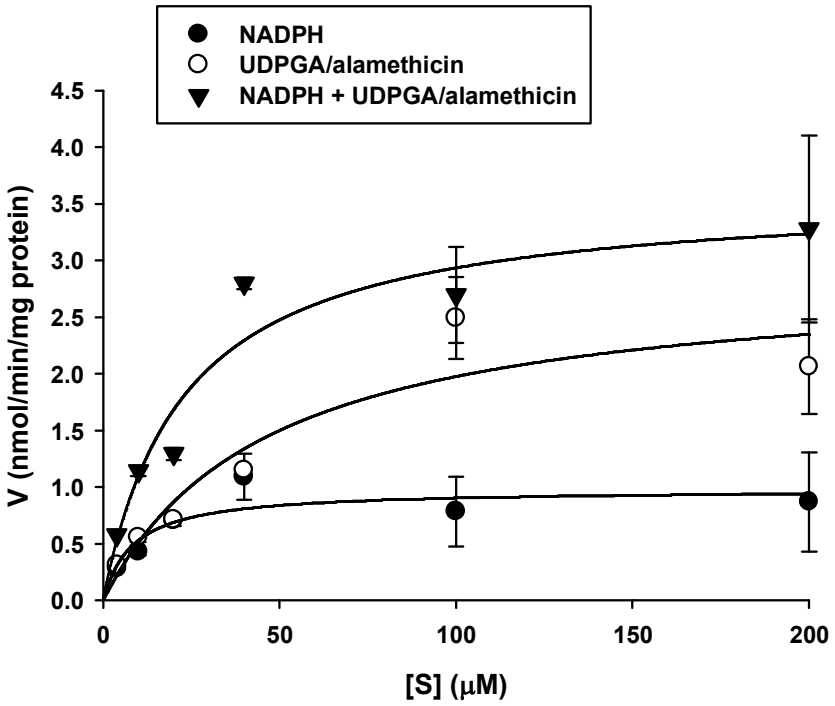

Figure 4. Concentration dependency for the metabolic reaction of MAG in RLM in the presence of either or both of NADPH and UDPGA/alamethicin (n = 3).

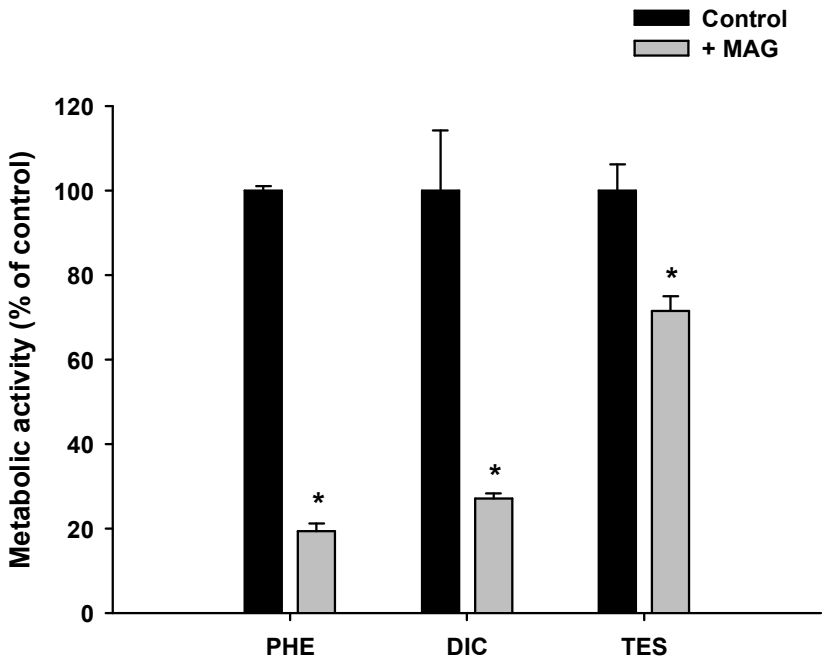

Figure 5. Effect of MAG on the metabolic reaction of PHE (CYP1A2), DIC (CYP2C9) and TES (CYP3A4) in HLM (n = 3). *, significantly different from the control group ($p < 0.05$).

(a)

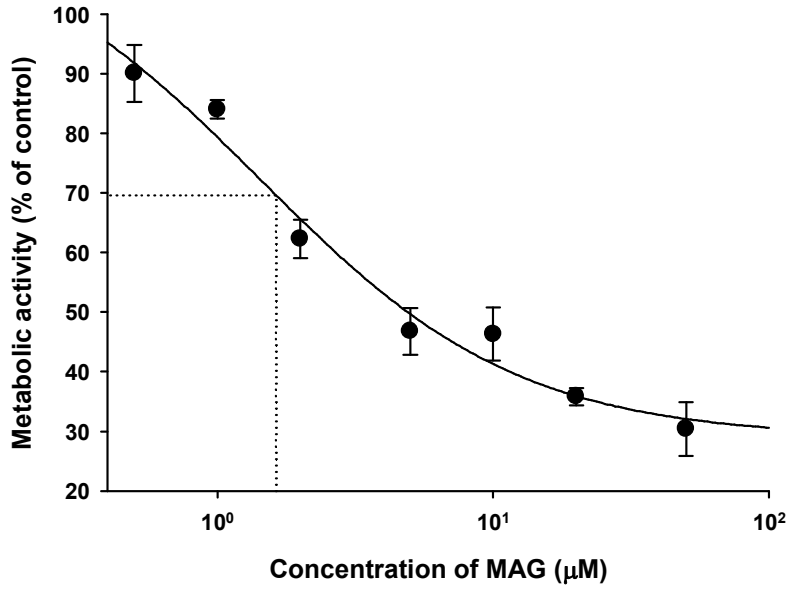
Metabolic activity (% of control)
100
90
80
70
60
50
40
30
20
10^0
10^1
10^2
Concentration of MAG (μM)

(b)

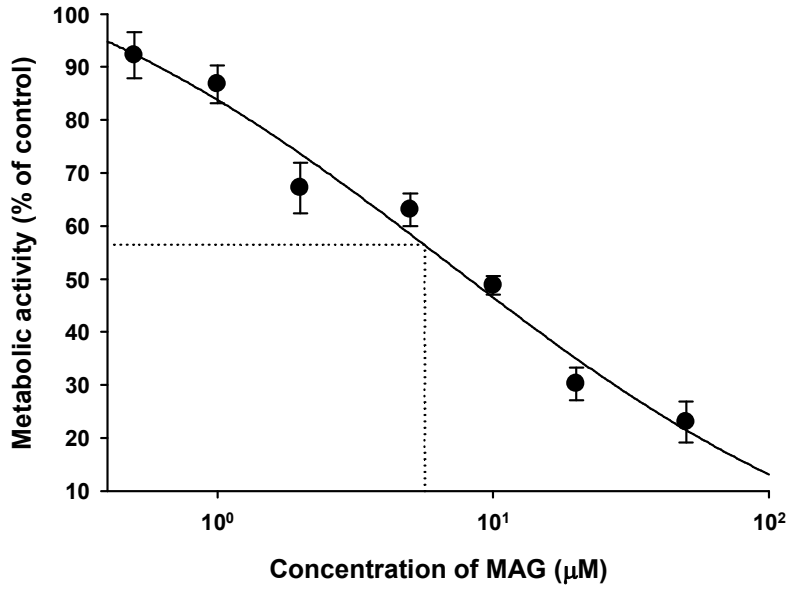
Metabolic activity (% of control)
100
90
80
70
60
50
40
30
20
10
10^0
10^1
10^2
Concentration of MAG (μM)

(c)

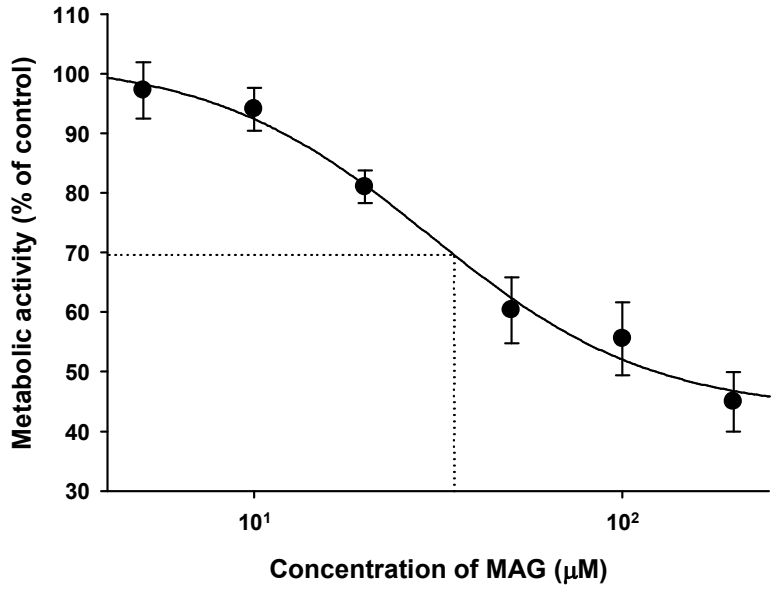

Figure 6. IC_{50} of MAG for the metabolic reaction of (a) PHE (CYP1A), (b) DIC (CYP2C) and (c) TES (CYP3A) in RLM (n = 3).

(a)

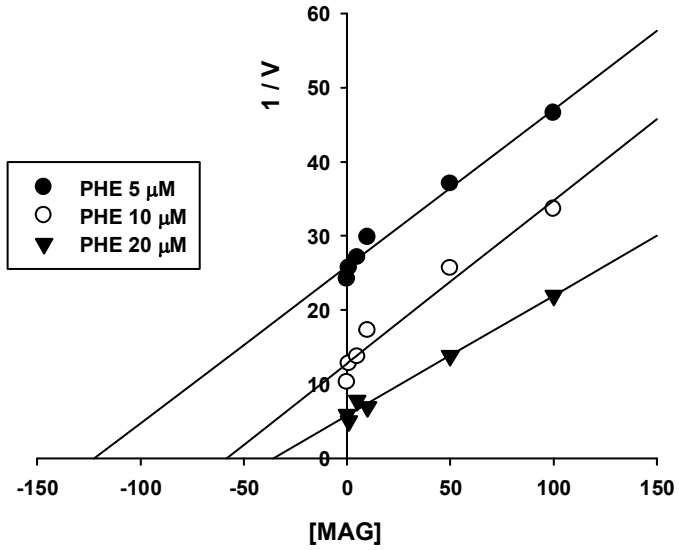
1 / V
60
50
40
30
20
10
0
-150
-100
-50
0
50
100
150
[MAG]
PHE 5 μM
PHE 10 μM
PHE 20 μM

(b)

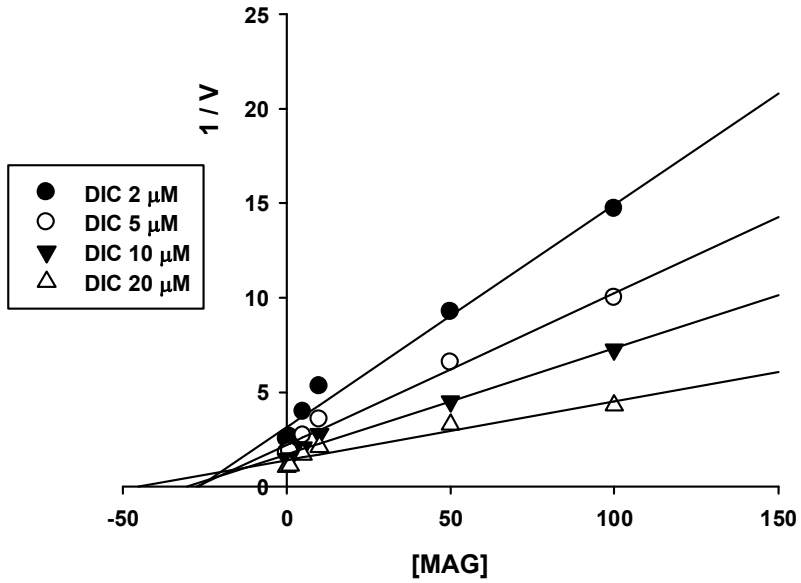
25
20
15
10
5
0
1 / V
DIC 2 μM
DIC 5 μM
DIC 10 μM
DIC 20 μM
-50
0
50
100
150
[MAG]

(c)

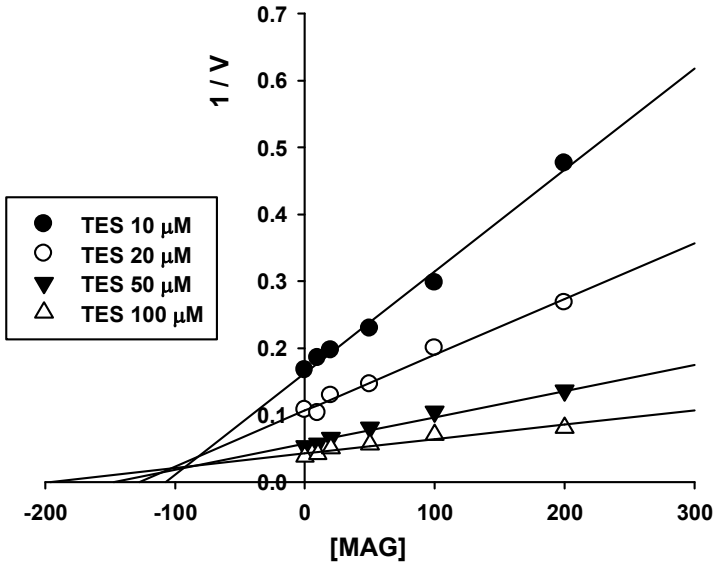

Figure 7. Representative Dixon plots for the inhibitory effects of MAG on the metabolic reaction of (a) PHE (CYP1A), (b) DIC (CYP2C) and (c) TES (CYP3A) in RLM.

국문초록

간 사이트크롬 P450 약물 대사에서 Puerarin 이 미치는 영향에 대한 연구

서울대학교 대학원

약학과 약제학 전공

김 상 범

Puerarin (PU, 8-β-D-glucopyranosyl-7-hydroxy-3-(4-hydroxyphenyl)-4H-1-benzopyran-4-one) 은 칡뿌리(kudzu root)에서 분리하여 얻어지는 주요 약리작용물질 중 하나이다. PU은 중국에서 심장혈관질환에서 임상적으로 정맥주사를 통해 처방되고 있다. 또한 여러 한약재의 처방에 빈번하게 사용되는 물질이다. 심장혈관질환을 갖고 있는 환자는 여러 약물의 동시복용가능성이 많음에도 불구하고, PU에 대한 약물상호작용은 연구가

충분치 않은 상황이다. 따라서, 본 연구를 통해 랫트와 인간의 간 사이토크롬 P450에 의한 약물 대사에서 PU이 어떤 영향을 주는지 밝히고자 하였다. 이를 위해 in vitro의 인간과 랫트 간 microsome을 통한 PU의 CYP enzyme 억제 효과를 평가하였다. 모델 기질은 FDA guidance을 참고하였으며, CYP1A2는 phenacetin (PHE), CYP2C9는 diclofenac (DIC), CYP2D6는 dextromethorphan (DEX) 그리고 CYP3A4는 testosterone (TES)을 기질로 하였다. CYP3A의 probe substrate인 buspirone (BUS)을 정맥주사와 경구로 각각 투여하였고, 이때 PU과 단회 정맥주사로 동시 투여하는 방식으로 in vivo 랫트에서 BUS의 약물동태를 평가하였다. In vitro CYP 억제 연구에서, 10-μM PU 의 존재조건에서 CYP3A4의 모델 기질 TES의 상대적 대사 활성이 유의적으로 감소하였으며, 이때 다른 CYP 기질들은 사람과 랫트 microsome에서 유의적인 영향이 없었다. 따라서 PU는 인간과 랫트에서 in vitro 간 CYP3A4 매개 대사를 억제한다고 생각할 수 있다. BUS (10mg/kg)을 PU (10mg/kg)의 용량으로 랫트에서 동시정맥주사로 투여하면, CL이 감소하면서 BUS의 AUC가 증가하였다. 반면에, BUS (10mg/kg)을 경구 투여하면서 정맥주사로 PU (10mg/kg)을 동시 투여하면, BUS의 AUC,

F(생체이용률) 값이 유의적으로 증가하였다. In vitro microsome과 in vivo 랫트의 약물 동태연구 결과, PU가 간 CYP3A4 매개 약물 대사의 억제 가능성이 있으며, 또한 그것의 기질인 경우 PU와 병용 투여시 임상적으로 중요한 허브와 약물의 대사매개 상호작용을 유발할 가능성이 있음을 알 수 있었다.

검색어: Puerarin, 사이토크롬 P450, 간 대사, 약물체내속도론, Buspirone, 랫트, 인간

학번: 2010-30463